

Impact of Artificial Roughness Enhancers on Solar Air Heater Performance: A Review

Vishal D Chaudhari[‡] 

[‡]Mechanical Engineering Department, Cusrow Wadia Institute of Technology, Pune, Maharashtra, India- 411038

vishaldchaudhari@gmail.com

Received: 21.07.2023 Accepted: 21.08.2023

Abstract- Solar air heaters have gained significant attention as an efficient and sustainable means of harnessing solar energy for various heating applications. However, adding artificial roughness to heat transfer surfaces enhances their performance. These roughness enhancers are strategically designed to improve heat transfer and increase the overall thermal effectiveness of the system. These roughness-enhancing geometries include rib roughness, vortex generators, wire coils, and various other configurations. The effects of these enhancers on pressure drop, heat transfer, and thermal performance are thoroughly analyzed and discussed. This review consolidates the existing knowledge in the field, presenting a comprehensive overview of the various roughness geometries, parameter ranges, and optimum data. The findings of the present work can act as a valued resource for investigators working on designing and optimizing air heating systems using solar energy.

Keywords Solar air heater, Thermo-hydraulic performance, Solar energy, Artificial roughness, SAH.

1. Introduction

The unwarranted consumption of fossil fuels is a grave concern and calls for immediate action. The challenge lies in finding alternate energy sources that will satiate the need for growing energy thirst without harming the environment. Fortunately, renewable energy sources are gradually emerging as the answer by developing alternate energy options like wind, solar, biomass, tidal, etc. Among these, solar energy stands out as the promising option that can lay the foundation for all other renewable energy sources. Solar thermal systems like solar air heaters harness the heat from solar radiation and provide hot air that can be further utilized for various applications. [1-3]

Solar air heaters can provide an economical and sustainable solution for harnessing solar heat energy to produce hot air. In recent years, solar air heaters have garnered significant attention as a viable alternative to traditional heating systems, primarily due to their potential to reduce energy consumption and carbon emissions. They have been utilized in applications like space heating, drying, industrial processes of heating or curing, etc. [4-7]. Continuous improvement is crucial for increasing the performance and efficiency of solar air heaters. The continuing advancement process supports solar air heaters to perform better, leading to amplified efficiency and more significant user benefits.

2. Performance Evaluation of SAH

In any SAH, the absorbing surface (plate) is a vital part where solar heat is absorbed and disseminated. A visual representation of a typical SAH is shown in Figure 1. The system's thermal efficiency can be directly improved by increasing the absorber surface. Many changes have been suggested and put into practice to increase the absorber plate's surface area, such as adding roughness obstacles and baffles, which not only increase the absorber plate's surface area but also encourage turbulence in the flow channel, improving heat transfer within the solar air heater and enhancing performance. [8-12]

An explicit performance evaluation must be carried out to produce an affordable and effective design for a solar air heater (SAH). This evaluation should examine essential performance indicators such as heat transfer coefficient, friction factor, and Nusselt number. These variables offer significant insights into the SAH's thermal effectiveness and thermo-hydraulic performance. The SAH performance often remains a function of its design parameters and requires a comprehensive review of the investigations carried out by the researchers in the field [13-16]. The objective of the current study is to survey the different heat augmentation methods employed to enhance the performance of solar air heaters. By synthesizing the collective knowledge from previous research, this study aims to develop more efficient and cost-effective SAH designs, thus fostering advancements in the

field and promoting the widespread adoption of this sustainable heating technology.

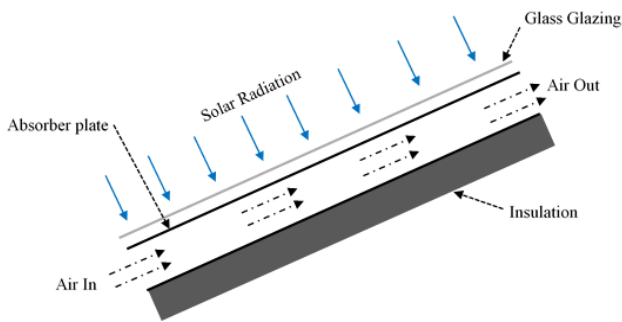


Fig. 1. Layout of solar air heater

2.1. SAH with Fins for Heat Transfer Enhancement

Sriromreun et al. [17] examined the effect of baffles mounted below the absorber in a zigzag arrangement, as presented in Fig. 2. The baffle introduction aims to promote turbulence creation using vortices that will lead to enhanced heat exchange. The distance between the baffles (pitch) and their height was varied, and the results were analyzed. It is noticed that the heat exchange (Nu) surges with decreasing pitch-to-height ratio of the baffle and increases by almost 300% to 400% compared to the heater plate without baffles. Compared to 0.5, 2, and 3, the baffle with a pitch ratio of 1.5 was observed to have the most significant frictional resistance factor.

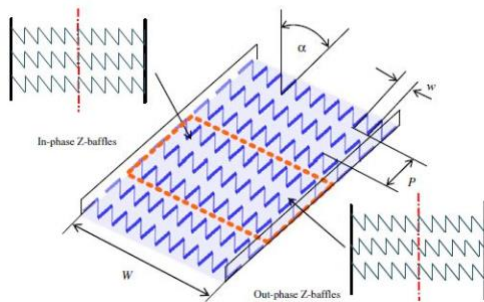


Fig. 2. “Z” baffles [17]

Absorber plates integrated with aluminum foam baffles having a porosity of about 85 % were studied by Bayrak et al. [18] for SAH applications (Fig. 3). The exergy and energy performance is calculated for varying flow rates of the air between 0.016 to 0.025 kg/s. In both cases, the baffles are arranged staggered and sequentially with a pitch of 6 mm and 10 mm. It was noted that the staggered baffles offered superior performance than the sequential provision. Moreover, baffles with a 6mm staggered layout gave a peak energy efficiency of 77% and an exergy efficiency of 54.5% at a 0.025 kg/s flow rate. Mahmood et al. [19] built single-pass and double-pass solar collectors integrated with wire mesh layers to enhance heat transfer. Aluminum fins were also installed in the flow rate path in the transverse direction. The air is circulated half an hour before the data recording to establish the flow. The maximum difference in temperature of about 45 °C is obtained in two pass arrangement at the lowest airflow of 0.011 kg/s, and the bed temperature

encountered is more in a double-pass arrangement due to preheating of the air. The maximum efficiencies calculated are 55% and 62.5% at 0.032 kg/s, i.e., peak flow condition. Besides, the efficiency of heat transmission in the case of a two-pass heater was found to increase with a reduction in the depth of the lower channel passage.



Fig. 3. Porous baffles [18]

Chabane et al. [20] conducted the experiment on SAH having fins (longitudinal-semi cylindrical) mounted beneath the absorbing surface, as represented in Fig.4. The testing was conducted for dual flow rates viz. 0.016 and 0.012 kg/s on absorbers with and without fins for varying collector thickness (0 to 0.1 m). The maximum average temperature of air (94.0 °C) is recorded for collector thickness of 0.02 m at 0.016 kg/s flow rate. The average absorbing surface temperature rises with the length but, after 1.1 m, becomes stagnant. The highest heat exchange efficiency of 51.5 % is recorded at 0.16 kg/s later in the day. Priyam et al. [21] tested SAH by having a wavy finned absorber plate to comprehend the influence flow rate of air and spacing between the fins. With a surge in air flow rate across the board and for total fin spaces, the overall heat loss for wavy finned structure decrease additionally, a more considerable fin spacing results in increased heat loss. The solar collector efficiency rises as the overall heat exchange area is improved by narrowing the fin spacing. The heat removal factor also escalates with air flow rate and reduced fin spacing. The optimum results were obtained for minimum fin spacing of 1 mm at a flow rate of 0.013 kg/s. Mahboub et al. [22] built and tested SAH with a curved channel for air flow with a convex-shaped absorber. The thermal effectiveness and pressure drop rose with the airflow rate. Thermal efficiency shows an increases up to a flow rate of 0.046 kg/m²; after this, the enhancement is marginal. It is attributed to no further rise in heat losses from the collector. The effective efficiency considering thermal and hydrodynamic aspects was found to have a maximum value of 75 % at the 0.045 kg/m² air discharge.

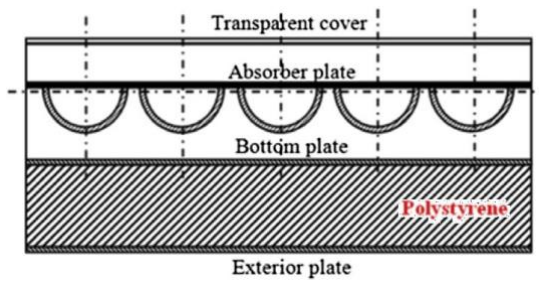


Fig. 4. Semicylindrical fins [20]

Sahu et al. [23] studied the influence of the angle of attack and roughness pitch on the thermal efficacy of SAH. The experimentation was carried out for airflow rates ranging between 0.01 kg/s to 0.4 kg/s. The absorber plates having pitch (roughness) values of 15, 10, and 8 were used, and the angles of attack tested were 40°, 60°, and 75°. The thermal efficiency increased by almost 40% to 69% when the air flow rate from 0.01 kg/s to 0.4 kg/s; the increase in the angle of attack was initially found to increase the performance but then decreased. The maximum efficiency is observed at the angle of attack for 60° and attributed to vortices formation and flow separation due to roughened ribs. The pressure drop declines with a pitch (roughness) rise and attack slope. Sivakandhan et al. [24] modified the SAH duct (rectangular) to have a rectangular air flow path in the upper section and a triangular flow path in the lower area. The influence of rib roughness properties like pitch ratio, height ratio, and arc angle on the system performance is examined. The heat transmission efficiency for a modified duct with roughness was better than a modified duct without roughness and a plain rectangular duct with lower mass flow rates. But at a mass flow rate greater than 0.04 kg/s, though the trend is identical, the efficiency for modified duct without roughness and plain vent decreases. Below 0.04 kg/s flow rate, the attack angle and roughness height have negligible effect on the system's efficiency. As studied previously, Kumar et al. [25] developed a SAH setup with an absorber unit with three walls roughened compared to single wall roughening. The top border had multiple V- grooving while the side walls were embedded with transverse wires. The effect of varying roughness pitch and attack angle is studied on the system's performance, and the best combination is found. An enhancement of about 50% in air temperature was recorded with SAH having three walls roughened compared to a single fence roughened unit, though with an increase in length, the change among the two was found to diminish. Maximum efficiency is recorded for three walls roughened unit for attack angle of 60° and pitch value of 10. For Reynolds's number greater than 12000, the efficiency variation between single-side and multiple-side roughened units was shrinking. The low time of stay in the chamber at high flow rates was predicted as a cause for reducing the difference in thermal efficiency.

The exergy and energy study for SAH having arc-shaped fins was performed by Ghritlahre [26]. The investigation is conducted for upstream and downstream flow layouts with roughened absorber plates, and the outcomes are compared to smooth flow. It has been revealed that upstream flow has better thermal efficiency than downstream flow. However,

exergy efficiency surpasses upstream efficiency later in the day. The roughened scales have better energy and exergy performance than smooth plates. It is endorsed to run the structure at a lower mass flow rate to have improved performance. MesgarPour et al. [27] studied triangular channel cross-section air heaters having helical paths for airflow numerically and experimentally. From the experimental analysis, the authors reported that higher flow rates have improved efficiency because of enhanced flow rate and heat transfer. Besides, though efficiency was found to have an inverse trend with solar radiation, the maximum efficiency is obtained at peak radiation input. The coefficient of heat transfer has also increased due to increased flow and a more significant differential between the in and out air temperatures. The average thermal efficiency calculated was 41.8% and 55.3% for airflow rates of 0.019 kg/s and 0.026 kg/s. The improved heat transfer was credited to the creation of vortices in the helical pathway. A maximum error of 3 % is observed between numerical and experimental performance. Numerical results have predicted that after the seventh helix (out of 10), the temperature differential is negligible so that absorber length can be curtailed to this point.

SAH with corrugate absorber plates and the built-in receiver was tested by El_Said et al. [28]. During testing, the inclination was changed from 0° to 20° with step 5° while flow rates between 11 l/s to 25 l/s were tried. With the increase in inclination, the average efficiency (thermal) increases due to more utile energy yield. Also, the rise in air flow rate creates turbulence and helps to increase heat transmission. The airflow dominated the inflow and outflow temperature differential more than the tilt angle. The reduced residence period of air in the heating chamber at higher flow and tilt angle was observed to affect the thermal effectiveness negatively. The higher power requirement at increased flow rates decreases the thermo-hydraulic efficacy at high flow rates. The study acclaims an optimum tilt angle of 20° and a flow rate of 25 l/s.

2.2. SAH having Absorber with Obstacles in Air Flow Path

Bekele et al. [29] examined the SAH's delta-shaped obstacles in the airflow path as represented in Fig. 5. The obstacle height is determined considering the flow blockage (maximum 75% and minimum 25%), while the pitch is decided based on the flow separation. Compared to the friction factor augmentation rate, the heat transfer enhancement rate is more significant when the relative obstacle height is 0.50 compared to 0.75 and 0.25. For the Re number range under study, the best performance is obtained at an angle of 30°, and it is attributed longer stay of the air in the duct at lower grades. A test section having V- grooved absorber plate on which centrally punched delta wings are mounted, was built by Skullong et al. [30]. The effect of V-groove's forward and backward arrangement at different attack angles is studied. The outlet air temperature is higher in the forward groove design than in the back groove design. The heat transmission experienced in bold groove design is more elevated than in backward groove at the highest attack angle values. Compared with smooth channels, the grooved

design found more thermal enhancement. Though there is an increase in heat transfer, friction loss also increases with the groove design of the absorber plate. The friction loss with no hole in the delta wing arrangement is comparable to a wing with a hole.

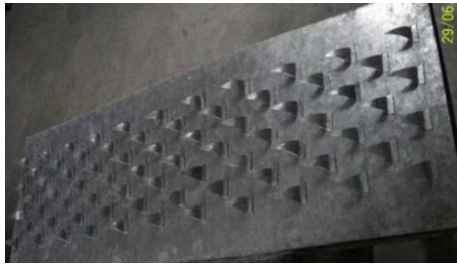


Fig. 5. Delta obstacles [29]

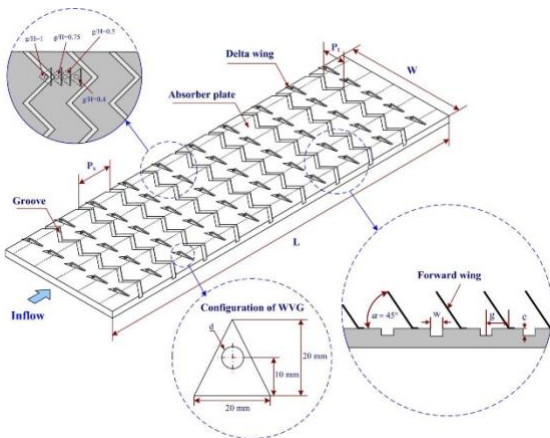


Fig. 6. Delta wing vortex generators [30]

Rajaseenivasan et al. [31] conducted a study to understand the improvement in the performance of SAH with absorbers equipped with turbulators of circular and V-section sections. Six different arrangements of V and circular sections were tested, as shown in Fig. 7. Thermal enhancement was found to be decreasing in all cases with Reynolds number. The maximum thermal enhancement is recorded for type F, where V inserts in the circular section have to reason to create more turbulence.

Bhattacharya et al. [32] probed the influence of forward turbulence generators on the augmentation of heat exchange in solar air heaters. The tabulator used has pitch ratios of 3.0, 4.0, and 5.0, while attack angles of 10°, 20°, and 30° were employed during the testing. It is revealed that the inclination angle has a higher impact on the Nusselt number and thermal

enhancement factor than the pitch ratio. The Nusselt number falls with the pitch ratio and rise with the increase in attack angle. Compared with the flow without turbulence generators, more significant deviations in friction factors are observed at higher values of Reynold Number values. In contrast, a more substantial variation was observed at lower Reynolds number values in the case of friction factor. Phu et al. [33] built a SAH with helically wound metal shaving for heat transfer enhancement. The experimentations were conducted for Reynolds's number varying from 5000 to 25000 (step of 5000), and the effect of relative roughness pitch (RRP) and relative roughness height (RRH) is understood. Owing to the development of recirculation zones behind the shaving, the heat transfer is detected to rise. With the decrease in RRP, the Nu number increases, and the maximum Nu is obtained at an RRP of 4.7. The RRH of 0.26 (minimum) provided the highest Nu number for an RRP of 4.7. However, the best thermo-hydraulic performance (THP) is obtained for RRP of 4.4 and RRH of 0.35. Ambade et al. [34] examined the performance of symmetrical gap and staggered element arrangement of ribs on the heat transfer through SAH. The relative rib pitch varies from 6 to 14, and the maximum helpful heat gain is obtained for a 10. Contrarily the leading friction factor is observed at the same angle. As expected, the thermo-hydraulic performance shows a similar behavior: it rises until ten and then decreases.

A flow domain comprised of quarter-circular and half-trapezoidal ribs located on solar air heater absorbing plates was built and tested by Singh et al. [35]. A 16.6% and 13.3% increase is observed in the temperature factor for trapezoidal and quarter circular ribs, respectively. The Nusselt number decreases marginally for trapezoidal ribs compared to triangular ribs. The trapezoidal profiled ribs have a lower pressure drop for the triangular profile, owing to less flow obstruction. Bensaci et al. [36] designed SAH having different rectangular baffle positioning and tested it for thermal-hydraulic performance. The scenarios tested include baffle located in the initial half, later half, and all over the absorber, as presented in Fig. 8. The Nusselt number was maximum when baffles were found all over the absorber, while it was minimum when baffles were positioned in the latter section of the absorber. Lower dead zones and increased flow mixing are reasons behind the rise in Nusselt number. The THPP was found to have a maximum value (0.7) for a 100% baffle-occupied absorber. Still, it is also stated that a rise in heat transfer cannot beat the bank in friction factor.



Fig. 7. Circular and V-inserts [31]

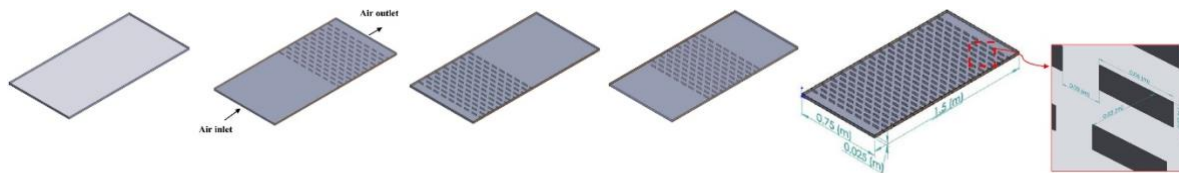


Fig. 8. Varying baffle filling ratio [36]

Solar air heater having rectangular section integrated with baffle blocks of V geometry was built and analyzed by Pandey et al. [37] to maximize heat exchange efficiency (Fig. 9). The baffle block shapes V up, and V down had angles of 30° and 45°. The findings revealed that air jets released from perforations induce turbulence leading to a significant rise in Nusselt number and pressure difference. The friction factor values in the V-up frame are observed to be slightly on the lower end compared to the V-down frame. The Baffle block with a V-up arrangement offered a % thermal efficiency of 96% at a roughness height of 0.7 and a relative pitch of 6.

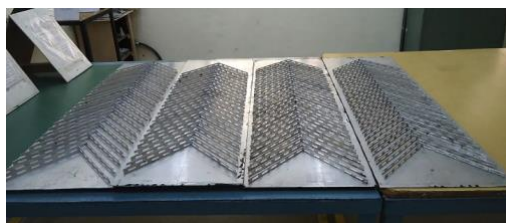


Fig. 9. V baffle blocks [37]

Parsa et al. [38] inspected the effectiveness of SAH having cuboid baffles, presented in Fig. 10. The aluminum baffles are placed on stainless steel absorber sheet such that the preceding baffle will direct the flow toward the succeeding baffle. The introduction of baffles was found to mix the flow and resulted in vortex formation. This resulted in heat transfer enhancement compared to flow over the smooth plate. But with rising Reynolds's number, the Nusselt number enrichment decreases. The thermo-hydraulic performance for baffled SAH was more excellent by 17.5 % compared to previous layouts. The investigation for exergy and energy creation of SAH, having an absorber equipped with L-type protrusions, was performed by Dulaimi et al. [39]. The arrangement is depicted in Fig.11. The experiments were conducted for single and double lines of ribs at air speeds of 0.9, 1.7, and 1.9 m/s. Inclusion of fins has raised the air outlet temperature from 48 to 50 °C, 49 to 52 °C, 52 °C to 57 °C for flow velocities of 1.9, 1.7, and 0.9 m/s, correspondingly. The maximum efficiency obtained with two line fins at 1.9 m/s was about 80%.

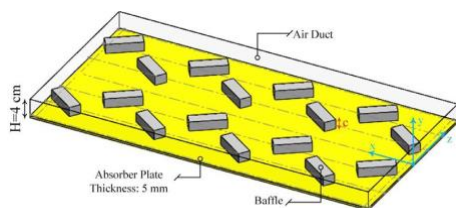


Fig. 10. Cuboid baffles [38]



Fig. 11. L shape fins [39]

Mahmood et al. [40] studied the impact of ribs (multiarc) attached below the absorbing plate on the effectiveness of SAHs. The geometric parameters like gap number, pitch ratio, and rib height are shuffled for Reynolds's number varying from 200 to 20000, and its effect was recorded. The useful heat gain and thermal efficiency increase with rib height, gap number between the ribs, and Reynold's number. The thermal efficiency increases with increasing pitch ratio up to a ratio of 12, beyond which it starts to decline. For all variations, the performance of an absorber plate with a multiarc rib is superior to a smooth plate absorber. The optimum performance is observed for a rib height of 0.045, having three gaps, and a pitch ratio of 12. Nidhul et al. [41] investigated SAH having inclined baffles and walls with semi-cylindrical surfaces. The purpose of the study to understand the influence of location of gap between the baffles, beneath the absorber surface (Figure 12). The range of 0.6 to 1 and 6000 to 14000, is utilized for baffle pitch (relative) Reynolds number during the study. The arrangement having gaps at trailing apices provided the optimum thermo-hydraulic effectiveness of 2.69. The corresponding baffle pitch and Reynolds number is 0.75 and 3000 respectively.

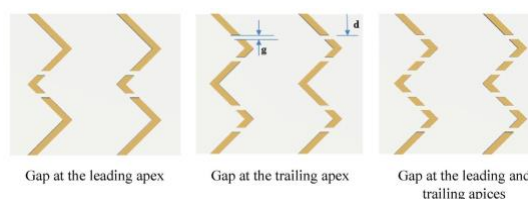
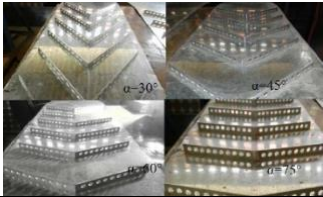
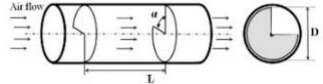
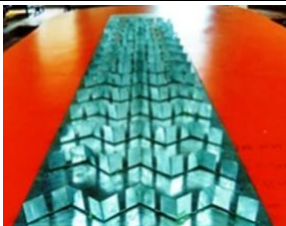
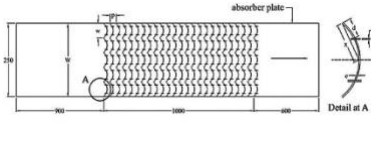
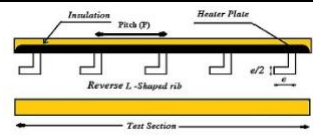
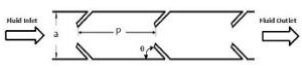
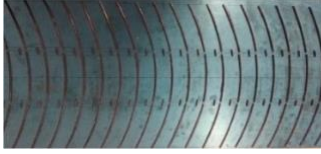
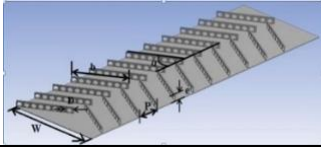
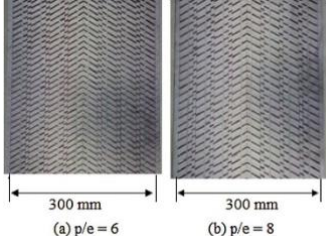
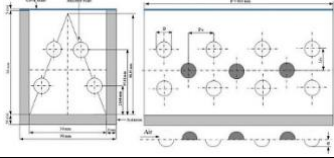
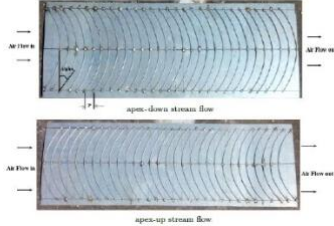


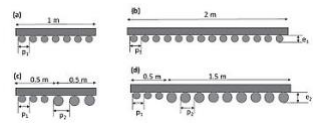
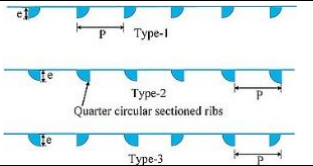
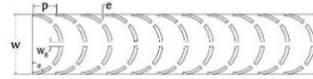
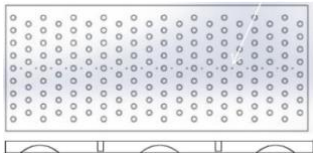
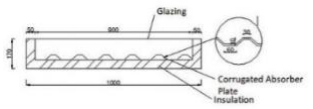
Fig. 12. Inclined baffles with gap [41]

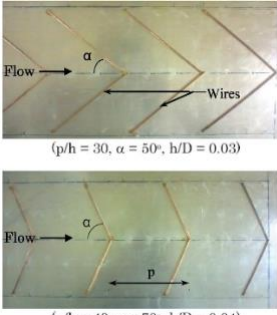
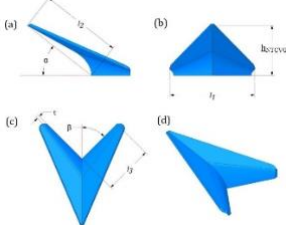
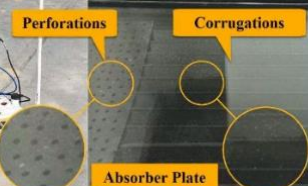
Table 1 summarizes the various types of fins/rib designs, specifically artificial roughness geometries, which have been investigated. The table includes information on the range of parameters considered and the optimal data for these parameters.

Table 1 Various SAH performance enhancement studies by researchers

Researcher	Protrusion type	Geometry	Parameters	Result and optimum parameters
Alam et al. [42]	V-shaped perforated baffles		Reynolds number (Re): 2000 to 20000 The angle of attack (α): 30° to 75°	Highest Thermo-Hydraulic Performance Factor (THPP) of 3 observed at $\alpha = 60^\circ$ and Re of 2000
Acir et al. [43]	Circular turbulators		Pitch ratio (PR) 2, 2.8, 3.5 Angle ratio (AR) 0.125, 0.25, 0.375 Re: 3000 and 7500	Maximum thermal performance factor 2.9 in the PR = 2 and AR = 0.125 at Re of 3000
Kumar et al. [44]	Broken multiple V-type baffle		Re: 3000 to 8000 Relative baffle width: 1 to 6	Highest thermal performance for relative baffle width of 5.0 and Re of 3000
Pandey et al. [45]	Circular arcs with a 2 mm gap		Relative roughness pitch (P/e): 6 to 20 Angle of attack (α): 15° to 75° Re: 3600 to 15,100	Maximum THPP of 3.6 at P/e of 8, α of 60°, Re of 21000
Gawande et al. [46]	L shaped ribs		P/e: 7.14 to 17.8 Re: 3800 to 18000	Maximum THPP of 1.9 at P/e 7.14, Re 15000
Sawhney et al. [47]	Wavy-up delta winglet vortex generators		Delta winglets properties: Wave number (ϕ): 3 to 7 Relative Pitch (longitudinal) (P/H): 3 to 6	Optimum THPP of 2.09 for P/H of 3 and $\phi = 5$
Rajendran et al. [48]	V-up perforated baffles		With and without baffles Air flow rate: 0.02078 kg/s, 0.02778 kg/s, 0.0346 kg/s	Max efficiency of 89.3% attained for baffled absorber at 0.0346 kg/s flow rate.
Bhattacharyya et al. [32]			Pitch ratio: 3, 4, 5 Inclination angle: 10°, 20°, 30°	A thermal enhancement factor of 5.4 for Pitch ratio three and inclination of 30°
Kabeel et al. [49]	Longitudinal Fin (height)		Fin height: 3, 5 and 8 cm Air flow rate: 0.013 to 0.04 kg/s.	Maximum daily efficiency 57% for fin height 8 cm at 0.04 kg/s flow rate

Priyam et al. [50]	transversely positioned wavy fins		Air flow rate: 0.00312 to 0.0158 kg/s Fin spacing: 2 to 6 cm	Maximum efficiency 69.55% for 2 cm fin spacing at 0.0158 kg/s airflow
Ambade et al. [34]	Arc geometry: Symmetrical gap and staggered element		Relative rib pitch: 6, 8, 10, 12 and 14 Re: 3000–15000	Maximum thermo-hydraulic parameter of 1.41 at rib pitch of 10 at Re 11000
Jain et al. [51]	V-shaped perforated baffles		Relative blockage height: 0.3 to 0.6 Re: 4000 to 18,000	Highest THPP of 2.24 at relative blockage height 0.4 and Re 4000
Phu et al. [33]	Metal shavings turned on a steel shaft		Roughness pitch (relative): 4.7 to 9.4 Re: 5000 - 25000 Roughness height: 0.26 to 0.43	Maximum THPP of about 1.5 at Re of 19000 for 1.7 roughness pitch and 0.35 roughness height (relative)
Baissi et al. [52]	Curved delta-shaped baffles (perforated and non-perforated)		Relative longitudinal length :3 to 5 Relative transversal length:0.6 to 1 Re: 2500 to 12,000	Maximum TEF of 2.26 at the relative longitudinal length of 0.3 and relative transversal length of 0.6 for perforated arrangement
Patel et al. [53]	V- rib geometry		Rib pitch to height: (p/e) of 14, 12, 10, 8 and 6 Re 4000 to 14500	Maximum THPP for P/e of 10 and Re of 12364
Taha et al. [54]	Herringbone metal foam fins		Corrugation angle: 30°, 60°, 90° Air flow rate: 0.01 to 0.05 m³/s.	Maximum thermal efficiency of 87.7% at corrugation angle of 30° and 0.04 m³/s flow rate
Neno et al. [55]	V- Corrugated absorber plate formed dimple		Dimple dia.:5, 7, 9 mm Airflow : 0.006, 0.004, 0.002, 0.001 kg/s	Maximum efficiency of 65.7 % for 9 mm dimple for a flow rate of 0.006 kg/s
Sahu et al. [23]	Arc-shaped geometry- apex upstream and downstream		Relative pitch (P/e): 8 - 15 Air flow rate: 0.01 to 0.047 kg/s Angle of attack: 45 to 75°	Maximum thermal efficiency 69.2 % in upstream arrangement at 8 P/e, 60° attack angle, and 0.01 kg/s flow rate

Sureandhar et al. [56]	Arc rib fin arrangement : Fixed and variable		Absorber length: 2 m and 1 m Airflow rate: 0.02 to 0.06 kg/s	Maximum efficiency (79%) for 1m absorber length at 0.06 kg/s for variable rib fin
Mahanand et al. [57]	Quarter-circular ribs		Re: 3800 to 18000 Relative roughness pitch: 7.14 to 17.86	Maximal thermal enhancement ratio 1.88 for relative roughness pitch of 7.14
Mushatet et al. [58]	Rectangular fins		Rectangular rib heights: 1, 2, and 3 cm Air flow rate: 0.01559 to 0.042 kg/s	Optimum efficiency at 3cm rib height and 0.01559 kg/s flow rate
Aliabadi et al. [59]	Delta winglet tapes		Re: 1643 to 8215 Pitch: 12.5 to 37.5 mm (high to low and low to high) Height: 5, 10, 15 mm (high to low and low to high)	Maximum Overall Performance Index of 1.46 Reynolds number of 1643 for uniform pitch and height high to low
Mahmood et al. [40]	Discrete multi-arc (DMAR) ribs		Number of gaps (N_g) = 1 to 4 Rib height (e/D) = 0.018 to 0.045 Gap width (W_g/e) 0.5 to 2 Rib pitch (p/e) = 4 to 16 Angle of attack 30° to 75°	Optimum efficiency at p/e 16, e/D 0.045, W_g/e 1, N_g 3, and 75° for DMAR
Bhushan et al. [60]	Dimpled absorber plate		Flat and dimpled absorber Mass flow rates: 0.028 to 0.051 kg/sec	Maximum instantaneous efficiency obtained (76 %) at 0.76 kg/s flow rate for dimpled absorber
Ambika et al. [61]	Corrugated absorber		Air flow rate: 0.06, 0.14, 0.17, 0.25, 0.3 kg/s	Maximum efficiency of 64 % at 0.25 kg/s

<p>Abulkhair et al. [62]</p>	<p>Wire-roughened absorber plate</p>		<p>Wire pitch (p/h): 10, 20,30,40 Roughness height (h/D): 0.1,0.2,0.3,0.4 Flow approach angle (α) 20, 30, 50, 70, 90 Re: 3000 to 9000</p>	<p>Efficiency index 1.14 for wire roughened absorber. Re = 3000, $\alpha = 50^\circ$ p/h = 40, h/D = 0.01.</p>
<p>Obaid et al. [63]</p>	<p>Different shaped turbulators</p>		<p>Flat plate (F) Plate with rectangular (R), triangular (T), and circular (C) Inserts. Air flow rate: 0.0178 to 0.1 kg/s</p>	<p>Daily maximum efficiency 86% for rectangular inserts at 0.1 kg/s flow rate</p>
<p>Demirađ et al. [64]</p>	<p>Conic vortex generator</p>		<p>Attack angles (α): $45^\circ, 37.5^\circ, 30^\circ, 20^\circ$ Scale ratio (S): 0.6 to 1.4 :1 Angle of the blade (β): $60^\circ, 45^\circ, 30^\circ$</p>	<p>Highest thermal enhancement factor 1.316, at $\alpha=37.5^\circ, \beta=30^\circ$ and S=1:1,</p>
<p>Farzan et al. [65]</p>	<p>Porous and non-porous absorber</p>		<p>Porous and non-porous absorber Airflow rates - 0.012 and 0.024 kg/s</p>	<p>Maximum thermal efficiency 66.1 % in case of porous absorber with 0.0024 kg/s flow rate</p>

3. Conclusion

This review paper explored the role and effectiveness of artificial roughness enhancers (turbulators) in solar air heaters. A comprehensive analysis of existing literature and studies shows that artificial roughness plays a crucial role in enhancing the heat transfer characteristics and overall performance of solar air heaters. The following are the key features derived from the present review study:

- The inclusion of ribs, fins, or another type of insertions (turbulators) to increase the roughness of the absorber surface increases the turbulence of the air. It results in enhanced heat transfer and increased outlet temperature compared to a plain absorber.
- Presence of turbulators also increases the pressure drop across the heater box, and hence for analysis of the system, thermo-hydraulic performance is usually measured
- Along with the geometry of turbulators, their placement on the absorber plate is playing a vital role in performance improvement. This emphasizes the proper selection of relative roughness pitch, angle of attack, and relative roughness height.

- Air flow rate plays an essential along with turbulators in improving the performance of the solar air heater.
- Staggered arrangement of turbulators was found to perform better in inducing the turbulence and enhancing the heat transfer than inline arrangement.

Artificial roughness boosters can be employed as practical tools for improving the performance of solar air heater systems. Such systems offer promising solutions for sustainable energy use by fostering heat transfer and enhancing energy efficiency. Continued research and technological advancements in this area will contribute to the broader adoption of solar air heaters with artificial roughness, ultimately leading to a greener and more sustainable future.

References

[1] N. Sah and M. J. K. Mandapati, "Thermal performance of a double-pass solar air heater (SAH) with ribbed absorber surface – an experimental study," WJE, vol. 17, no. 3, pp. 373–380, March 2020.

[2] R. J. J. Molu, S. Dzonde Naoussi, P. Wira, W. Fendzi Mbasso, and S. Tsobzé, "Solar Irradiance Forecasting

- Based on Deep Learning for Sustainable Electrical Energy in Cameroon,” *International Journal of Smart Grid*, vol.7, no.2, June 2023.
- [3] V. D. Chaudhari, G. N. Kulkarni, and C. M. Sewatkar, “Mathematical modeling and computational fluid dynamics simulation of cabinet type solar dryer: Optimal temperature control,” *J Food Process Eng*, vol. 44, no. 4, April 2021.
- [4] P. Dhirawani, R. Parekh, T. Kandoi and K. Srivastava, “Cost Savings Estimation for Solar Energy Consumption Using Machine Learning”, 11th International Conference on Renewable Energy Research and Application (ICRERA), Istanbul, Turkey, pp. 42-49, 18-21 September 2022.
- [5] K. Lentswe and A. Mawire, "Charging Energetic and Exergetic Evaluation of A Combined Solar Cooking and Thermal Energy Storage System," 11th International Conference on Renewable Energy Research and Application (ICRERA), Istanbul, Turkey, pp. 71-76, 18-21 September 2022.
- [6] V. D. Chaudhari, and V. A. Kolhe, “Thermal modeling of temperature for cabinet solar dryer,” *Journal of Postharvest Technology*, vol. 11, no. 2, pp. 79-87, June 2023.
- [7] M. H. Ahmed, “Performance of Solar Adsorption Cooling System with Different Solar Collectors Technologies,” *International Journal of Renewable Energy Research*, vol. 11, no. 2, June 2021.
- [8] M. E. Shayan, G. Najafi, F. Ghasemzadeh, “Advanced Study of the Parabolic Trough Collector Using Aluminum (III) Oxide,” *International Journal of Smart Grid*, vol.4, no.3, September 2020.
- [9] S. Kyaligonza and E. Cetkin, “Photovoltaic System Efficiency Enhancement with Thermal Management: Phase Changing Materials (PCM) with High Conductivity Inserts,” *International Journal of Smart Grid*, vol.5, no.4, December 2021.
- [10] P. J. Bezbaruah, R. S. Das, and B. K. Sarkar, “Thermo-hydraulic performance augmentation of solar air duct using modified forms of conical vortex generators,” *Heat Mass Transfer*, vol. 55, no. 5, pp. 1387–1403, May 2019.
- [11] S. P. Komble, G. N. Kulkarni, and C. M. Sewatkar, “Numerical model for solar drying mechanism of grapes using double glazed cabinet type solar dryer,” *J Food Process Engineering*, vol. 45, no. 10, October 2022.
- [12] R. Karwa, “Thermo-hydraulic performance of solar air heater with finned absorber plate forming multiple rectangular air flow passages in parallel under laminar flow conditions,” *Applied Thermal Engineering*, vol. 221, p. 119673, February 2023.
- [13] M. Yang, X. Yang, X. Li, Z. Wang, and P. Wang, “Design and optimization of a solar air heater with offset strip fin absorber plate,” *Applied Energy*, vol. 113, pp. 1349–1362, January 2014.
- [14] K. Goel, S. N. Singh, and B. N. Prasad, “Performance investigation and parametric optimization of an eco-friendly sustainable design solar air heater,” *IET Renewable Power Gen*, vol. 15, no. 12, pp. 2645–2656, September 2021.
- [15] W. H. Khalil, Z. A. H. Obaid, and H. K. Dawood, “Exergy analysis of single-flow solar air collectors with different configurations of absorber plates,” *Heat Trans. Asian Res.*, vol. 48, no. 8, pp. 3600–3616, December 2019.
- [16] R. S. Gill, V. S. Hans, and R. P. Singh, “Optimization of artificial roughness parameters in a solar air heater duct roughened with hybrid ribs,” *Applied Thermal Engineering*, vol. 191, p. 116871, June 2021.
- [17] P. Sriromreun, C. Thianpong, and P. Promvonge, “Experimental and numerical study on heat transfer enhancement in a channel with Z-shaped baffles,” *International Communications in Heat and Mass Transfer*, vol. 39, no. 7, pp. 945–952, August 2012.
- [18] F. Bayrak, H. F. Oztop, and A. Hepbasli, “Energy and exergy analyses of porous baffles inserted solar air heaters for building applications,” *Energy and Buildings*, vol. 57, pp. 338–345, February 2013.
- [19] J. Mahmood, L. B. Y. Aldabbagh, and F. Egelioglu, “Investigation of single and double pass solar air heater with transverse fins and a package wire mesh layer,” *Energy Conversion and Management*, vol. 89, pp. 599–607, January 2015.
- [20] F. Chabane, N. Moumami, and S. Benramache, “Experimental study of heat transfer and thermal performance with longitudinal fins of solar air heater,” *Journal of Advanced Research*, vol. 5, no. 2, pp. 183–192, March 2014.
- [21] Priyam and P. Chand, “Thermal and thermohydraulic performance of wavy finned absorber solar air heater,” *Solar Energy*, vol. 130, pp. 250–259, June 2016.
- [22] Mahboub, N. Moumami, A. Brima, and A. Moumami, “Experimental study of new solar air heater design,” *International Journal of Green Energy*, vol. 13, no. 5, pp. 521–529, April 2016.
- [23] M. K. Sahu, M. M. Matheswaran, and P. Bishnoi, “Experimental study of thermal performance and pressure drop on a solar air heater with different orientations of arc-shape rib roughness,” *J Therm Anal Calorim*, vol. 144, no. 4, pp. 1417–1434, May 2021.
- [24] C. Sivakandhan, T. V. Arjunan, and M. M. Matheswaran, “Thermohydraulic performance enhancement of a new hybrid duct solar air heater with inclined rib roughness,” *Renewable Energy*, vol. 147, pp. 2345–2357, March 2020.
- [25] D. Kumar and L. Prasad, “Experimental Investigation on Thermal Performance in Three-Sided Solar Air Heaters Having an Alignment of Multi-v and Transverse Wire Roughness on the Absorber Plate,”

- Journal of Solar Energy Engineering, vol. 142, no. 5, p. 051011, October 2020.
- [26] H. K. Ghritlahre, "An experimental study of solar air heater using arc shaped wire rib roughness based on energy and exergy analysis," Archives of Thermodynamics, vol. 42, no. No 3. The Committee of Thermodynamics and Combustion of the Polish Academy of Sciences and the Institute of Fluid-Flow Machinery Polish Academy of Sciences, pp. 115–139, 2021.
- [27] M. MesgarPour, A. Heydari, and S. Wongwises, "Geometry optimization of double pass solar air heater with helical flow path," Solar Energy, vol. 213, pp. 67–80, January 2021.
- [28] E. M. S. El-Said, M. A. Gohar, A. Ali, and G. B. Abdelaziz, "Performance enhancement of a double pass solar air heater by using curved reflector: Experimental investigation," Applied Thermal Engineering, vol. 202, p. 117867, February 2022.
- [29] Bekele, M. Mishra, and S. Dutta, "Performance characteristics of solar air heater with surface mounted obstacles," Energy Conversion and Management, vol. 85, pp. 603–611, September 2014.
- [30] S. Skullong, P. Promvong, C. Thianpong, and M. Pimsarn, "Thermal performance in solar air heater channel with combined wavy-groove and perforated-delta wing vortex generators," Applied Thermal Engineering, vol. 100, pp. 611–620, May 2016.
- [31] T. Rajaseenivasan, S. Srinivasan, and K. Srithar, "Comprehensive study on solar air heater with circular and V-type turbulators attached on absorber plate," Energy, vol. 88, pp. 863–873, August 2015.
- [32] S. Bhattacharyya, H. Chattopadhyay, A. Guin, and A. C. Benim, "Investigation of Inclined Turbulators for Heat Transfer Enhancement in a Solar Air Heater," Heat Transfer Engineering, vol. 40, no. 17–18, pp. 1451–1460, November 2019.
- [33] N. M. Phu, V. Tuyen, and T. T. Ngo, "Augmented heat transfer and friction investigations in solar air heater artificially roughened with metal shavings," J Mech Sci Technol, vol. 33, no. 7, pp. 3521–3529, July 2019.
- [34] J. Ambade and A. Lanjewar, "Experimental investigation of solar air heater with new symmetrical gap arc geometry and staggered element," International Journal of Thermal Sciences, vol. 146, p. 106093, December 2019.
- [35] P. Singh, Akshayveer, A. Kumar, and O. P. Singh, "Efficient design of curved solar air heater integrated with semi-down turbulators," International Journal of Thermal Sciences, vol. 152, p. 106304, June 2020.
- [36] C.-E. Bensaci, A. Moumami, F. J. Sanchez De La Flor, E. A. Rodriguez Jara, A. Rincon-Casado, and A. Ruiz-Pardo, "Numerical and experimental study of the heat transfer and hydraulic performance of solar air heaters with different baffle positions," Renewable Energy, vol. 155, pp. 1231–1244, August 2020.
- [37] R. Pandey and M. Kumar, "Efficiencies assessment of an indoor designed solar air heater characterized by V baffle blocks having staggered racetrack-shaped perforation geometry," Sustainable Energy Technologies and Assessments, vol. 47, p. 101362, October 2021.
- [38] H. Parsa, M. Saffar-Avval, and M. R. Hajmohammadi, "3D simulation and parametric optimization of a solar air heater with a novel staggered cuboid baffles," International Journal of Mechanical Sciences, vol. 205, p. 106607, September 2021.
- [39] M. J. Al-Dulaimi, Areej H. Hilal, Husam A. Hassan, and Faik A. Hamad, "Energy and Exergy Investigation of a Solar Air Heater for Different Absorber Plate Configurations," Int. J. Automot. Mech. Eng., vol. 20, no. 1, pp. 10258–10273, March 2023.
- [40] Mahmood, M. Safaa, and A. Farhan, "Impact of Discrete Multi-arc Rib Roughness on the Effective Efficiency of a Solar Air Heater," September 2022.
- [41] K. Nidhul, S. Kumar, A. K. Yadav, and S. Anish, "Influence of Rectangular Ribs on Exergetic Performance in a Triangular Duct Solar Air Heater," Journal of Thermal Science and Engineering Applications, vol. 12, no. 5, p. 051010, October 2020.
- [42] T. Alam, R. P. Saini, and J. S. Saini, "Experimental investigation of thermo hydraulic performance due to angle of attack in solar air heater duct equipped with V-shaped perforated blockages," IJRET, vol. 6, no. 2, p. 164, 2015.
- [43] Acir and İ. Ata, "A study of heat transfer enhancement in a new solar air heater having circular type turbulators," Journal of the Energy Institute, vol. 89, no. 4, pp. 606–616, November 2016
- [44] R. Kumar, A. Kumar, R. Chauhan, and M. Sethi, "Heat transfer enhancement in solar air channel with broken multiple V-type baffle," Case Studies in Thermal Engineering, vol. 8, pp. 187–197, September 2016.
- [45] R. Pandey and M. Kumar, "Efficiencies assessment of an indoor designed solar air heater characterized by V baffle blocks having staggered racetrack-shaped perforation geometry," Sustainable Energy Technologies and Assessments, vol. 47, p. 101362, October 2021.
- [46] V. B. Gawande, A. S. Dhoble, D. B. Zodpe, and S. Chamoli, "Experimental and CFD investigation of convection heat transfer in solar air heater with reverse L-shaped ribs," Solar Energy, vol. 131, pp. 275–295, June 2016.
- [47] J. S. Sawhney, R. Maithani, and S. Chamoli, "Experimental investigation of heat transfer and friction factor characteristics of solar air heater using

- wavy delta winglets,” *Applied Thermal Engineering*, vol. 117, pp. 740–751, May 2017.
- [48] V. Rajendran, H. Ramasubbu, K. Alagar, and V. K. Ramalingam, “Performance analysis of domestic solar air heating system using V-shaped baffles – An experimental study,” *Proceedings of the Institution of Mechanical Engineers, Part E: Journal of Process Mechanical Engineering*, vol. 235, no. 5, pp. 1705–1717, October 2021.
- [49] E. Kabeel, M. H. Hamed, Z. M. Omara, and A. W. Kandeal, “Influence of fin height on the performance of a glazed and bladed entrance single-pass solar air heater,” *Solar Energy*, vol. 162, pp. 410–419, March 2018.
- [50] Priyam and P. Chand, “Experimental investigations on thermal performance of solar air heater with wavy fin absorbers,” *Heat Mass Transfer*, vol. 55, no. 9, pp. 2651–2666, September 2019.
- [51] S. K. Jain, R. Misra, A. Kumar, and G. D. Agrawal, “Thermal performance investigation of a solar air heater having discrete V-shaped perforated baffles,” *International Journal of Ambient Energy*, vol. 43, no. 1, pp. 243–251, December 2022.
- [52] M. T. Baissi, A. Brima, K. Aoues, R. Khanniche, and N. Moumami, “Thermal behavior in a solar air heater channel roughened with delta-shaped vortex generators,” *Applied Thermal Engineering*, vol. 165, p. 113563, January 2020.
- [53] S. Singh Patel and A. Lanjewar, “Experimental and numerical investigation of solar air heater with novel V-rib geometry,” *Journal of Energy Storage*, vol. 21, pp. 750–764, February 2019.
- [54] S. Y. Taha and A. A. Farhan, “Performance augmentation of a solar air heater using herringbone metal foam fins: An experimental work,” *Int J Energy Res*, vol. 45, no. 2, pp. 2321–2333, February 2021.
- [55] S. Neno and D. Ichani, “Experimental Study of Collector Performance Solar Air Heater with Dimple Staggered Arrangement on a V-Corrugated Absorber Plate,” *IOP Conf. Ser.: Earth Environ. Sci.*, vol. 557, no. 1, p. 012008, August 2020.
- [56] G. Surendhar, G. Srinivasan, P. Muthukumar, and S. Senthilmurugan, “Performance analysis of arc rib fin embedded in a solar air heater,” *Thermal Science and Engineering Progress*, vol. 23, p. 100891, June 2021.
- [57] Y. Mahanand and J. R. Senapati, “Thermo-hydraulic performance analysis of a solar air heater (SAH) with quarter-circular ribs on the absorber plate: A comparative study,” *International Journal of Thermal Sciences*, vol. 161, p. 106747, March 2021.
- [58] K. S. Mushatet and R. A. Fayyad, “Experimental investigation for performance evaluation of solar air heater collector,” presented at the Proceeding of the 1st international conference on advanced research in pure and applied science (ICARPAS2021): 3rd Annual Conference of Al-Muthanna University/College of Science, Al-Samawah, Iraq, 2022, p. 020042..
- [59] M. Khoshvaght-Aliabadi, N. Naeimabadi, F. Nejati Barzoki, and A. Salimi, “Experimental and numerical studies of air flow and heat transfer due to insertion of novel delta-winglet tapes in a heated channel,” *International Journal of Heat and Mass Transfer*, vol. 169, p. 120912, April 2021.
- [60] Bhushan, R. Kumar, and A. Perwez, “Experimental investigations of thermal performance for flat and dimpled plate solar air heater under turbulent flow conditions,” *Solar Energy*, vol. 231, pp. 664–683, January 2022.
- [61] Madhavankutty Ambika, A. Ghimire, and S. Appukuttan, “Experimental Performance Analysis of a Corrugation Type Solar Air Heater (CTSAH),” *Energy Engineering*, vol. 119, no. 4, pp. 1483–1499, 2022.
- [62] H. Abulkhair, A. O. Alsaiani, I. Ahmed, E. Almatrafi, N. Madhukeshwara, and B. R. Sreenivasa, “Heat transfer and air flow friction in solar air heaters: A comprehensive computational and experimental investigation with wire-roughened absorber plate,” *Case Studies in Thermal Engineering*, vol. 48, p. 103148, August 2023.
- [63] Z. A. H. Obaid, I. D. J. Azzawi, and K. Azeez, “The experimental study of energy features for solar air heaters with different turbulator configurations,” *Heat Trans*, vol. 52, no. 2, pp. 1380–1394, March 2023.
- [64] H. Z. Demirağ, M. Doğan, and A. A. İğci, “The experimental and numerical investigation of novel type conic vortex generator on heat transfer enhancement,” *International Journal of Thermal Sciences*, vol. 191, p. 108383, September 2023.
- [65] H. Farzan and E. H. Zaim, “Thermal analysis of a new double-pass solar air heater using perforated absorber and porous materials: An experimental study,” *Thermal Science and Engineering*, vol. 38, pp. 101680, February 2023